Short- vs Long-range Elastic Distortion: Structural Dynamics of a [2x2] Tetrairon (II) Spin Crossover Grid Complex Observed by Time-Resolved X-Ray Crystallography

Jose de Jesus Velazquez-Garcia[a]*, Krishnayan Basuroy[a], Darina Storozhuk[a], Joanne Wong[b], Serhiy Demeshko[b], Franc Meyer[b], Robert Henning[c] and Simone Techert[ad]

[a]Photon Science - Structural Dynamics in Chemical Systems, Deutsches Elektronen-Synchrotron DESY, Notkestraße 85, Hamburg, 22607, Germany

[b]Institut für Anorganische Chemie, Georg-August-Universität Göttingen, Tammannstraße 4, Göttingen, 37077, Germany

[c]Center for Advanced Radiation Sources, The University of Chicago, Argonne National Laboratory, 9700 South Cass Ave, Lemont, Illinois, 90439, USA

[d]Institut für Röntgenphysik, Georg-August-Universität Göttingen, Friedrich-Hund-Platz 1, Göttingen, 37077, Germany

Synthesis

The complex grid **FE4** and its ligand were synthesized following the procedure reported in literature[1]. The crystallographic data for this paper can be obtained free of charge from The Cambridge Crystallographic Data Centre via www.ccdc.cam.ac.uk/data_request/cif. Deposition numbers: 2195543-2195550, 2195552-2195555, 2195574-2195582.

Ortep plots

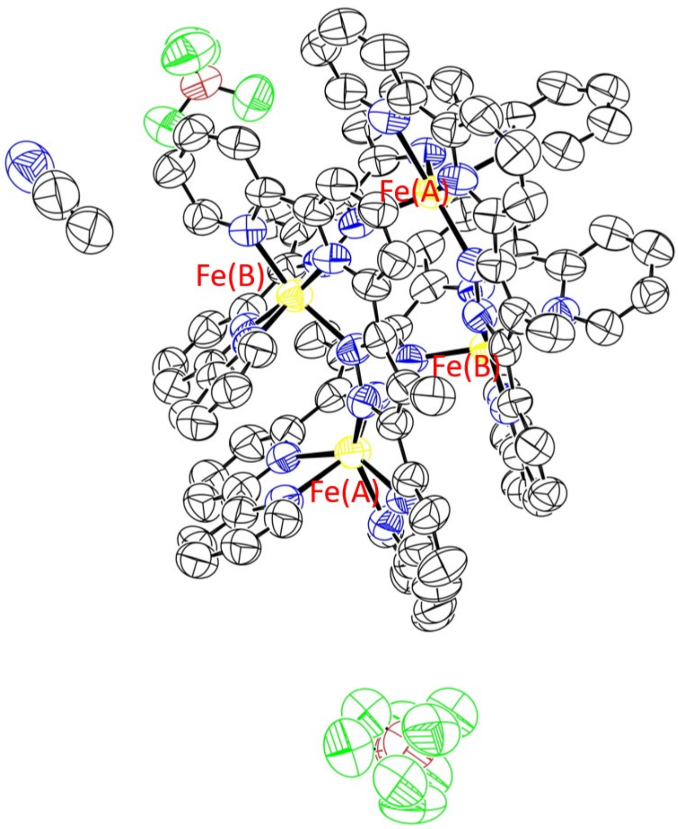

Figure S1. Thermal ellipsoid plot (50% of probability) for **FE4** for the -200*ps* data.

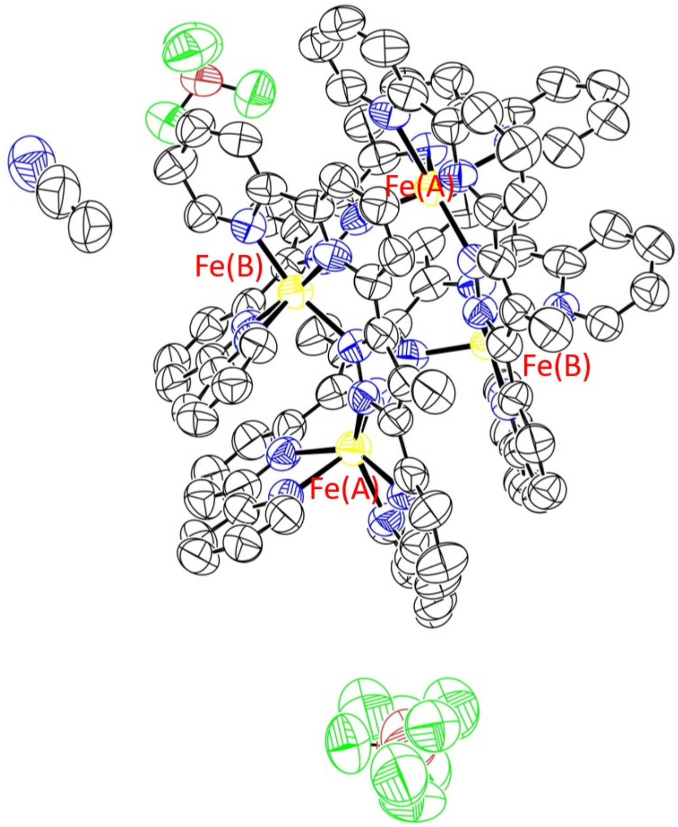

Figure S2. Thermal ellipsoid plot (50% of probability) for **FE4** for the 100*ps* data.

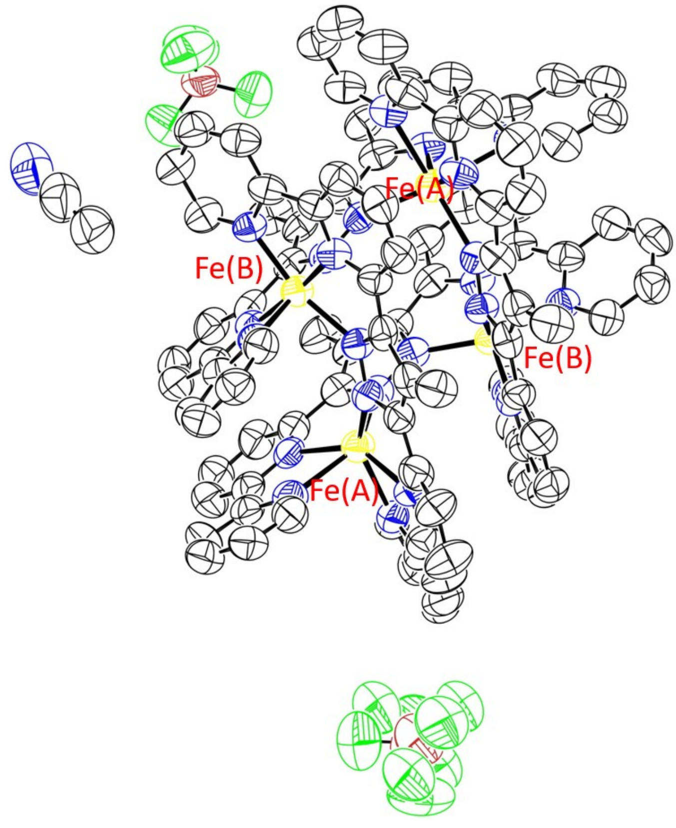

Figure S3. Thermal ellipsoid plot (50% of probability) for **FE4** for the 200*ps* data.

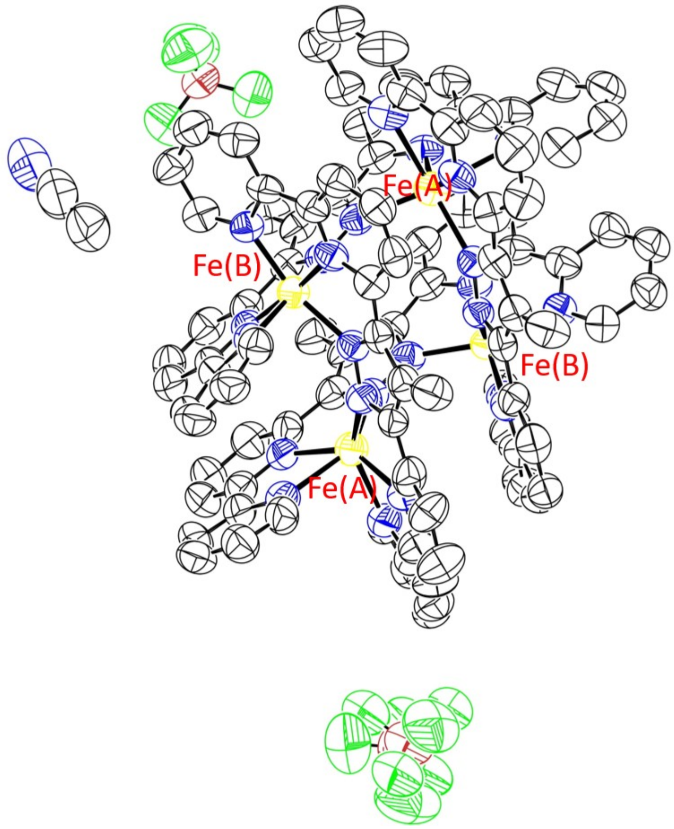

Figure S4. Thermal ellipsoid plot (50% of probability) for **FE4** for the 300*ps* data.

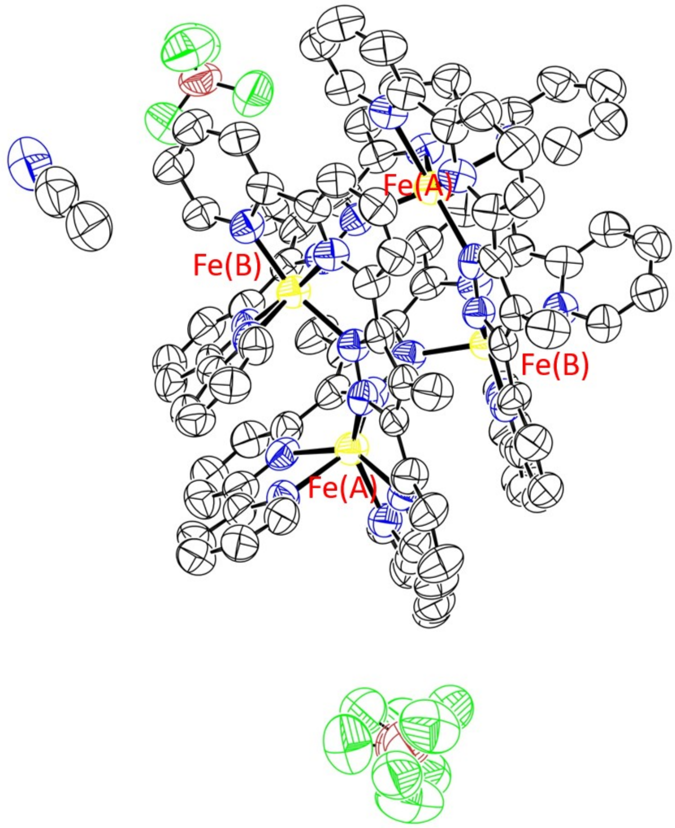

Figure S5. Thermal ellipsoid plot (50% of probability) for **FE4** for the 400*ps* data.

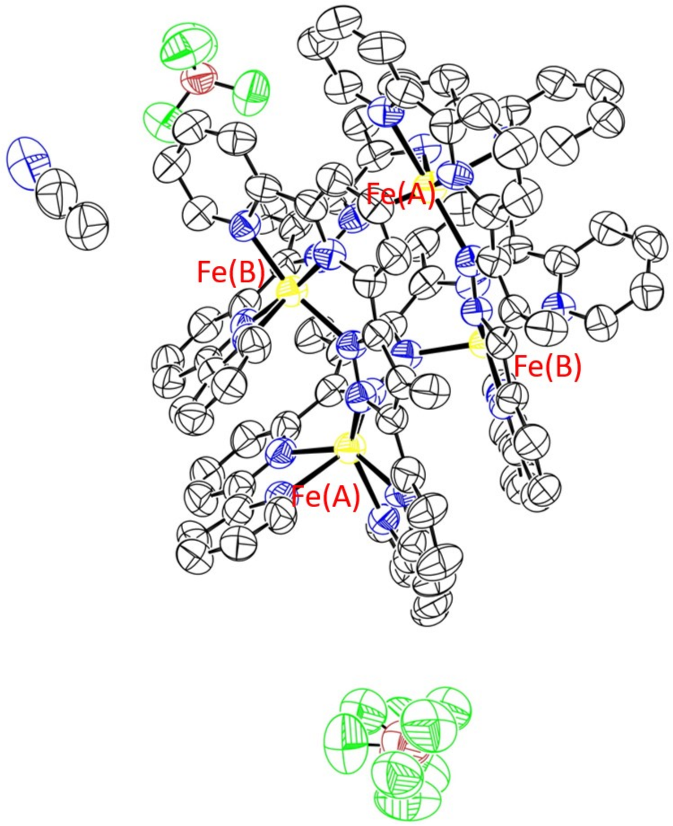

Figure S6. Thermal ellipsoid plot (50% of probability) for **FE4** for the 500*ps* data.

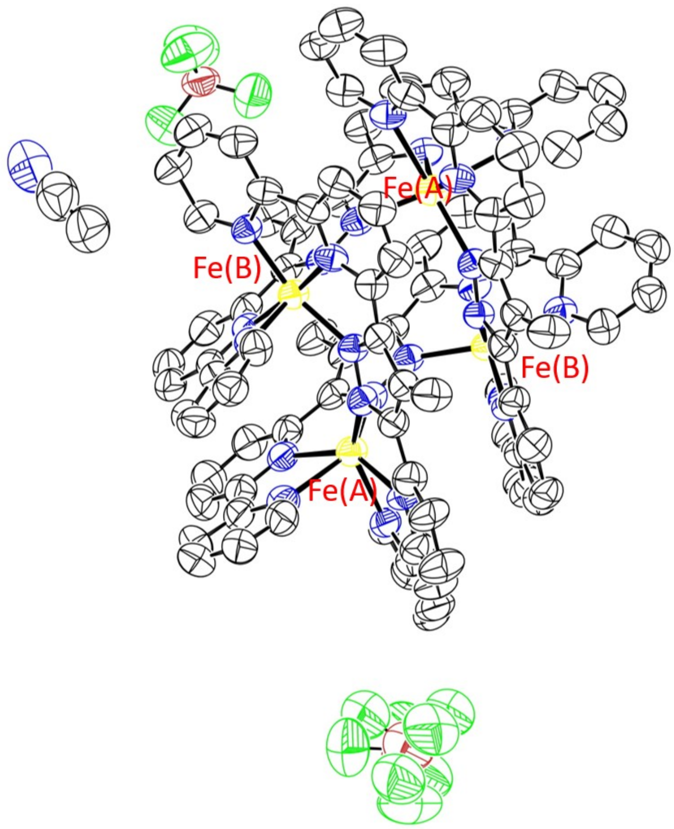

Figure S7. Thermal ellipsoid plot (50% of probability) for **FE4** for the 600*ps* data.

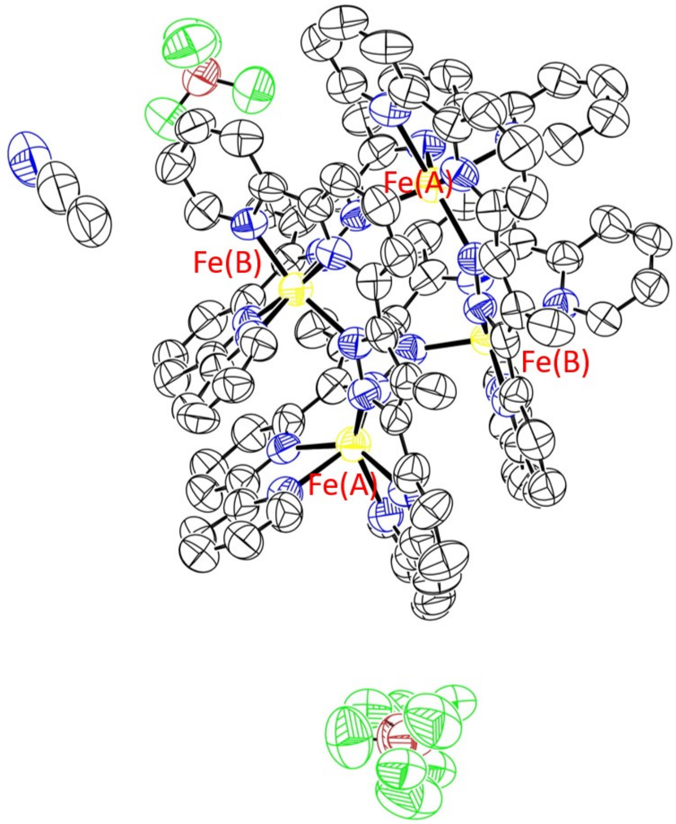

Figure S8. Thermal ellipsoid plot (50% of probability) for **FE4** for the 700*ps* data.

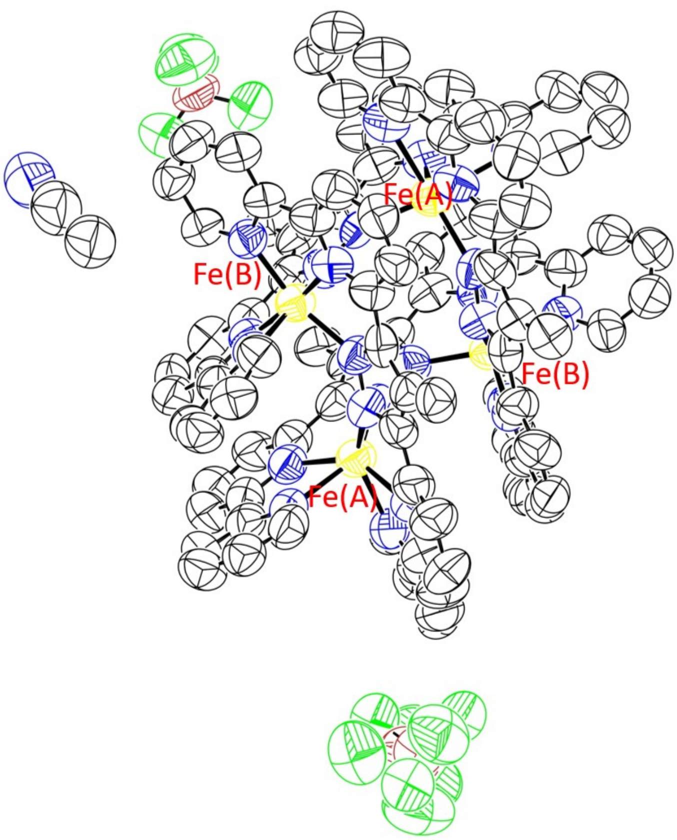

Figure S9. Thermal ellipsoid plot (50% of probability) for **FE4** for the 800*ps* data.

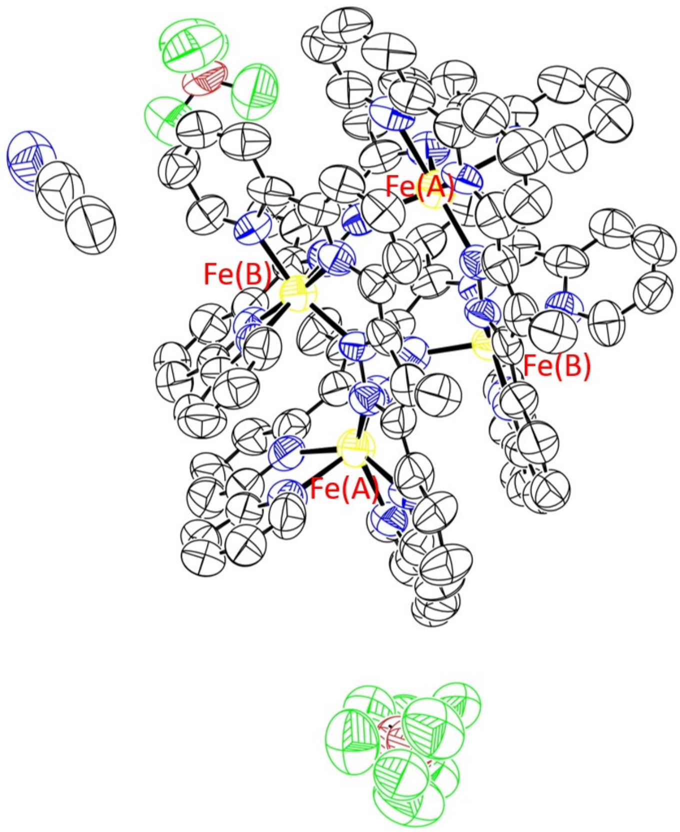

Figure S10. Thermal ellipsoid plot (50% of probability) for **FE4** for the 900*ps* data.

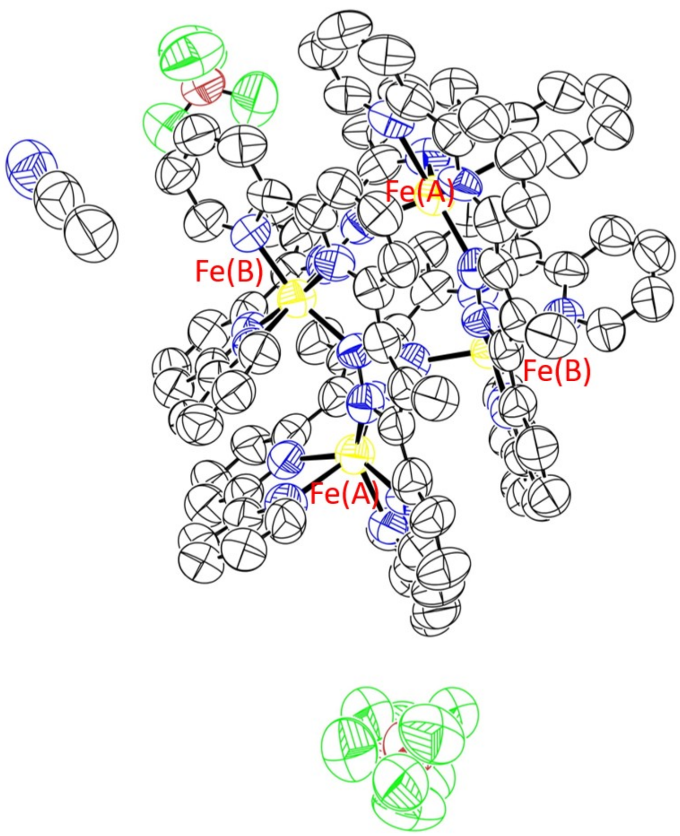

Figure S11. Thermal ellipsoid plot (50% of probability) for **FE4** for the 1*ns* data.

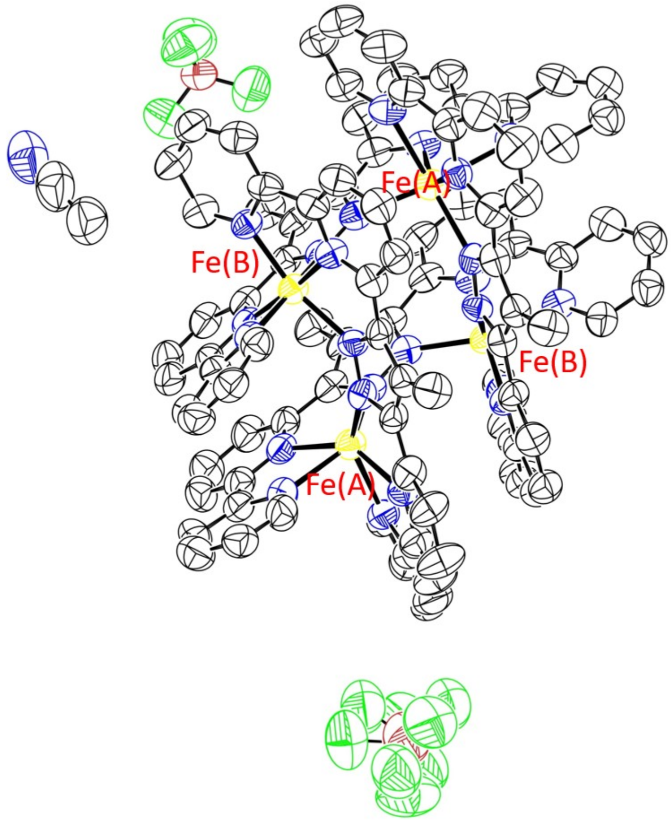

Figure S12. Thermal ellipsoid plot (50% of probability) for **FE4** for the 10*ns* data.

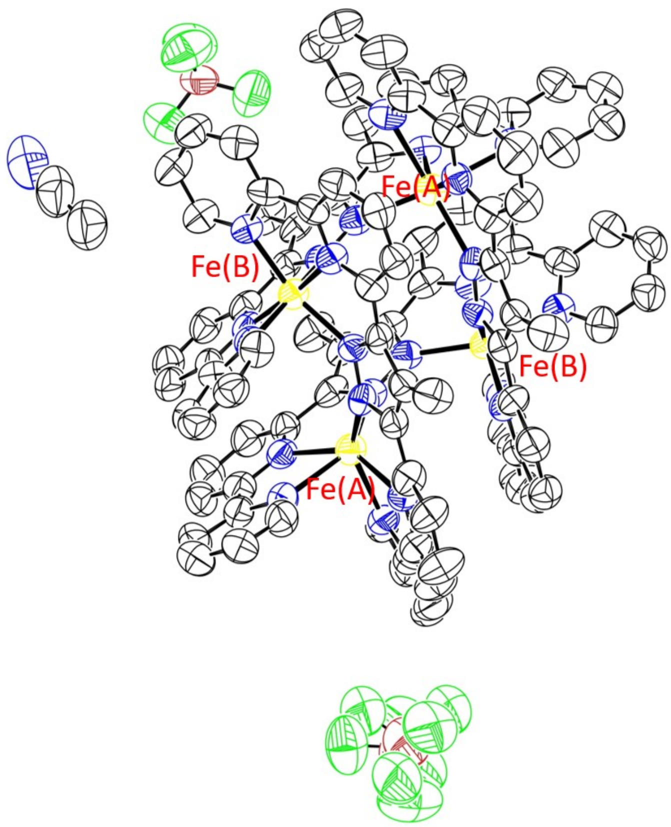

Figure S13. Thermal ellipsoid plot (50% of probability) for **FE4** for the 50*ns* data.

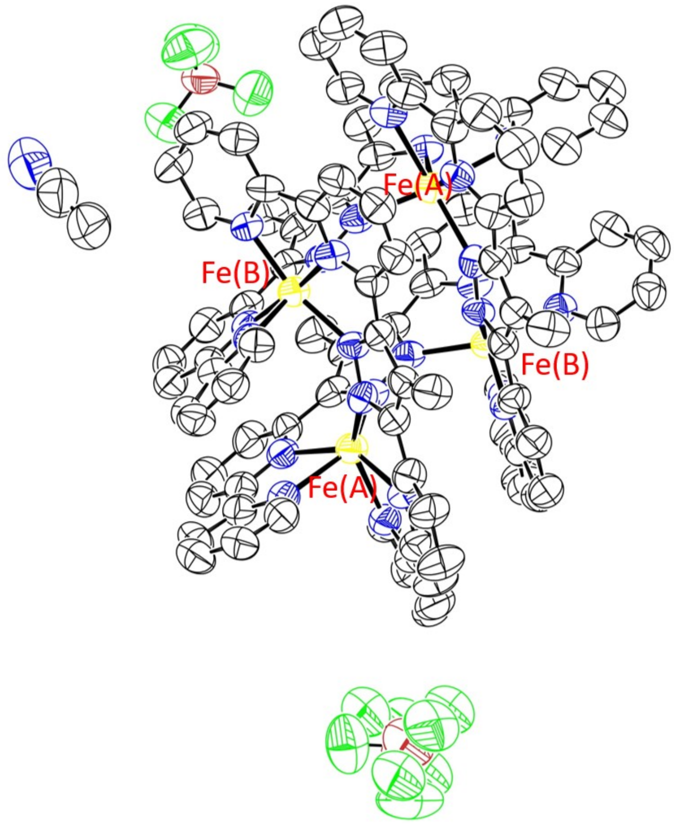

Figure S14. Thermal ellipsoid plot (50% of probability) for **FE4** for the 100*ns* data.

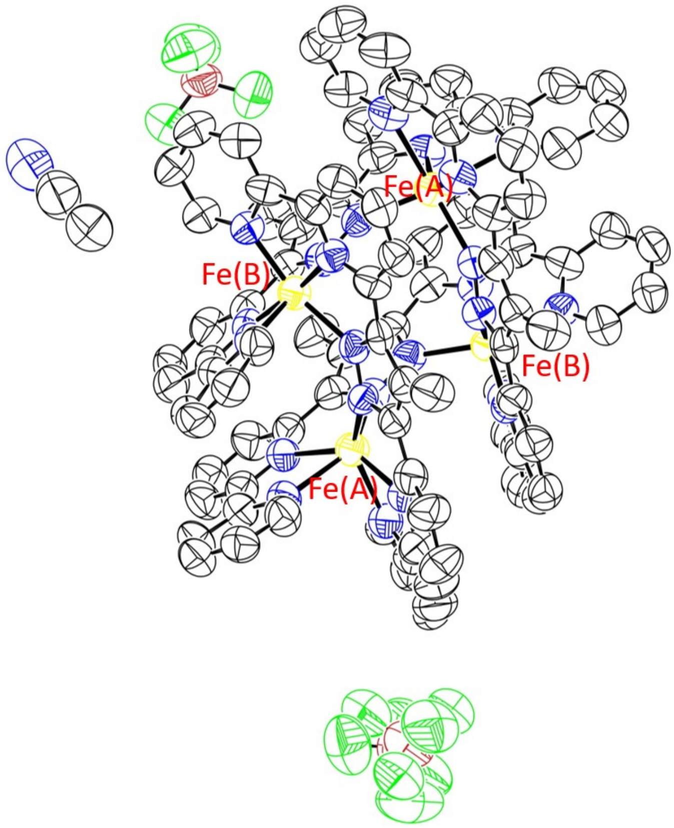

Figure S15. Thermal ellipsoid plot (50% of probability) for **FE4** for the 200*ns* data.

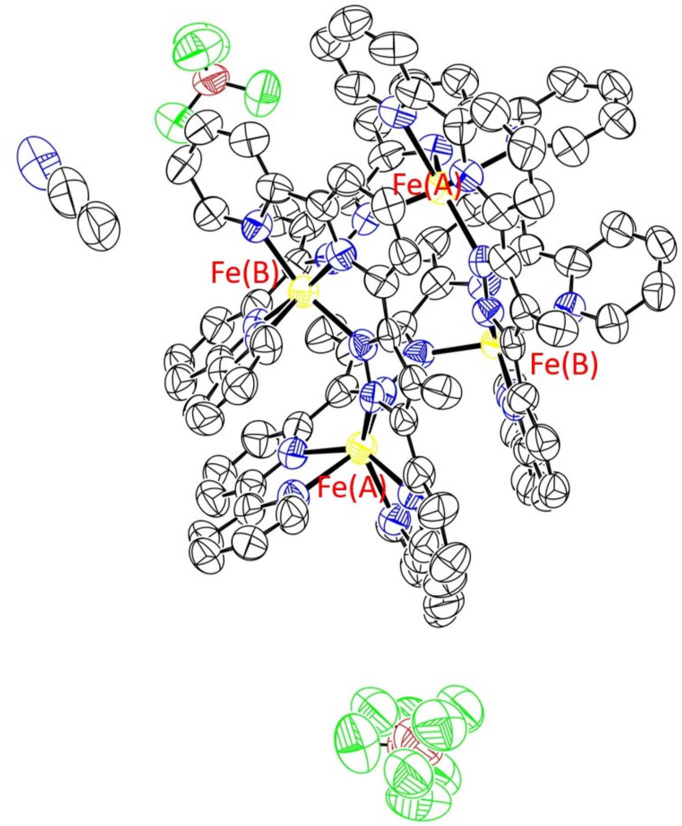

Figure S16. Thermal ellipsoid plot (50% of probability) for **FE4** for the 500*ns* data.

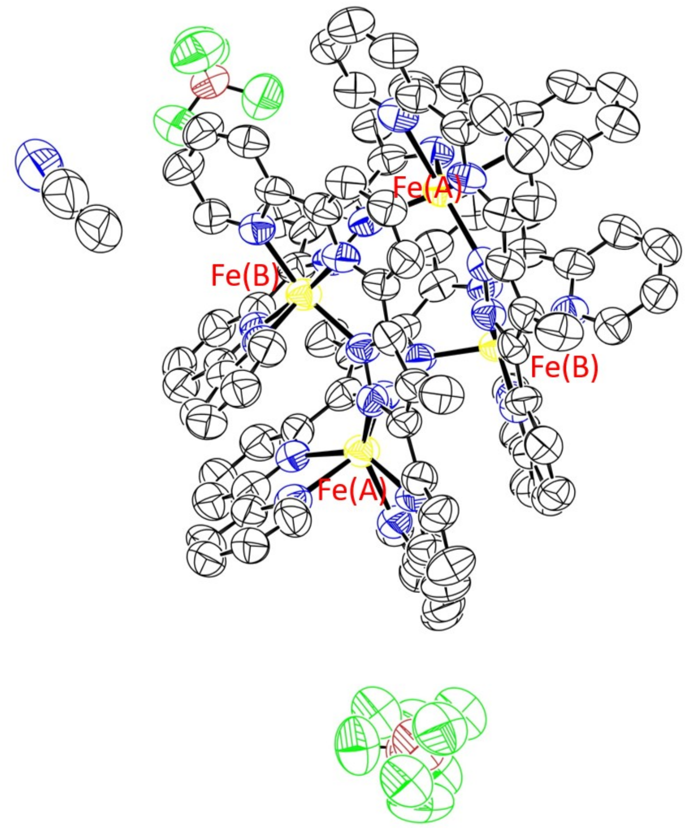

Figure S17. Thermal ellipsoid plot (50% of probability) for **FE4** for the 800*ns* data.

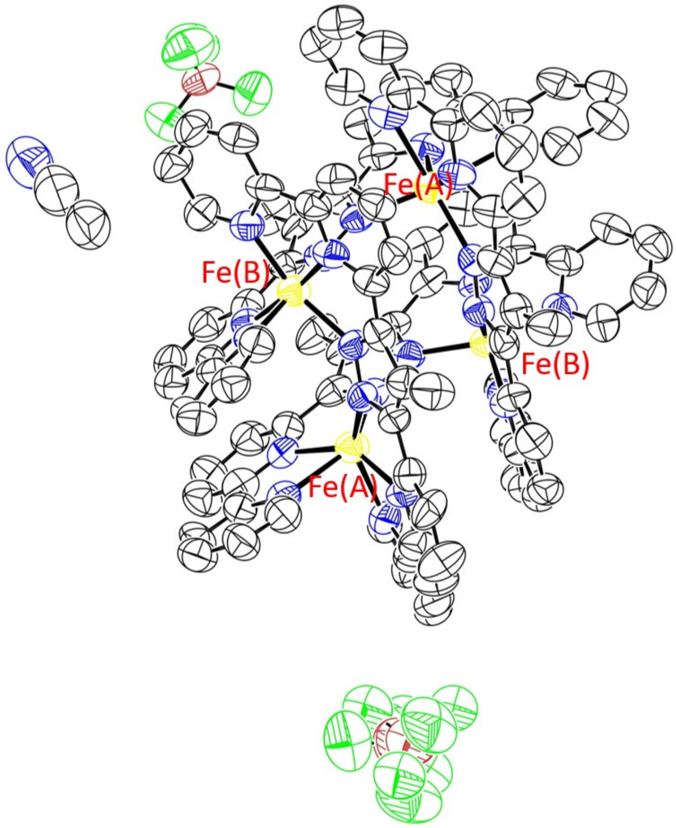

Figure S18. Thermal ellipsoid plot (50% of probability) for **FE4** for the 1μs data.

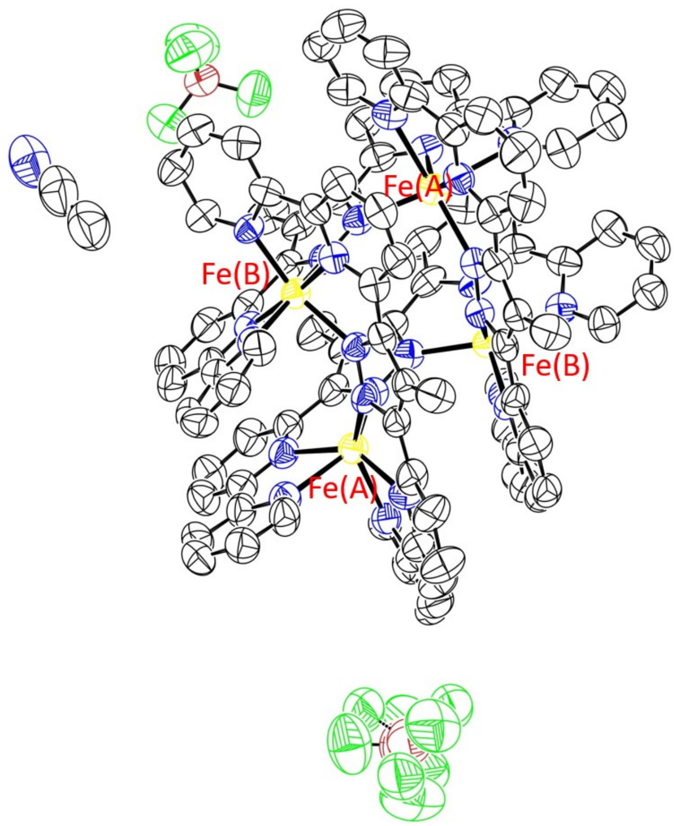

Figure S19. Thermal ellipsoid plot (50% of probability) for **FE4** for the 10μs data.

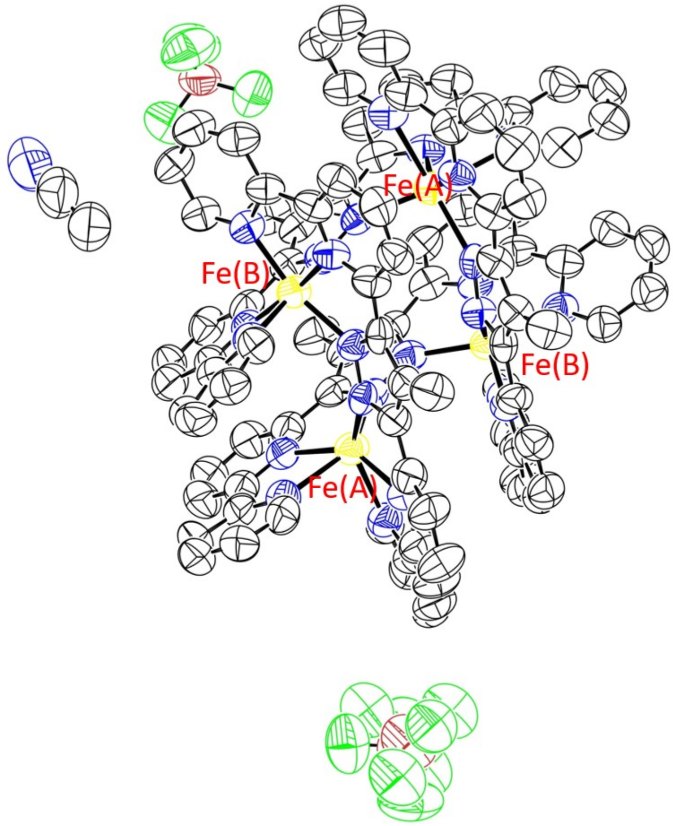

Figure S20. Thermal ellipsoid plot (50% of probability) for **FE4** for the 50μs data.

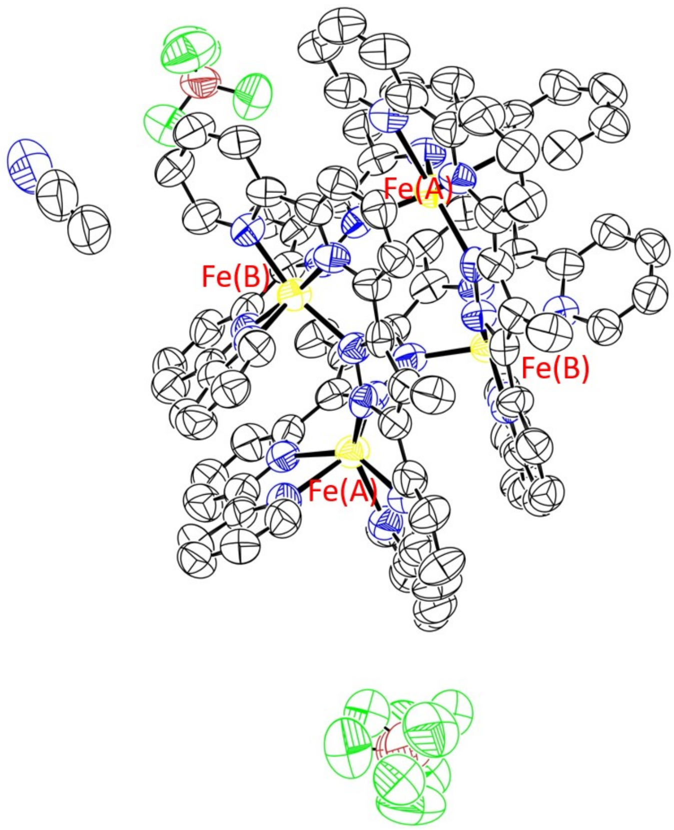

Figure S21. Thermal ellipsoid plot (50% of probability) for **FE4** for the 100μs data.

Structural Analysis

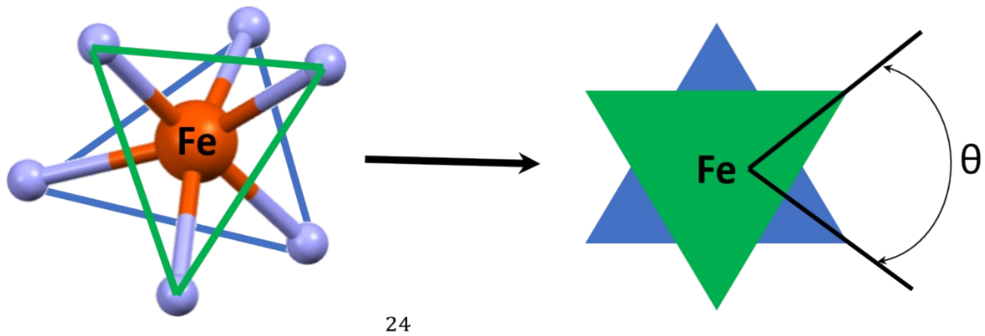

$$\Theta = \sum_{i=1}^{24}(|60 - \theta_i|)$$

Figure S22. Environment of Fe^{II} ions and definition of the θ angle and the angular distortion parameter (Θ).[2,3]

Temperature difference

The well-known Wilson plot[4] is frequently used to estimate the scale factor, k_S, and the overall isotropic temperature factor (B) of a data set. This plot can be obtained by statistical comparison of the observed intensities (I_{obs}) with the average squared structure factor equals $\sum_{i=1}^{M} f_i^2$ for each sin θ/λ range according to:

$$\ln\left(\frac{I_{obs}}{\sum_{i=1}^{M} f_i^2}\right) = \ln\left(k_s\right) - 2B(\sin\theta/\lambda)^2 \qquad \text{(S1)}$$

Where M is the number of atoms and , f_i is the scattering factor of the ith atom.

The change in the overall isotropic temperature factor (ΔB) between two data sets at different temperature can be estimated from modified Wilson plots. The plots are obtained by a scale-factor refinement of the low temperature data (e.g. 220K) with the high-temperature data (e.g. 250K) structural model and plotting the $\ln(I^{250K}/I^{220K})$. The slope of the dependence of $\ln(I^{250K}/I^{220K})$ with $(\sin\theta/\lambda)^2$ gives the overall increase of isotropic atomic motion, ΔB (equation S2), which is associated with temperature difference between the data sets.[5]

$$ln\left(\frac{I^{250K}}{I^{220K}}\right) = -2\Delta B^{250K-220K}(\sin\theta/\lambda)^2 \qquad \text{(S2)}$$

The greater the temperature difference between data sets the greater the value of ΔB, that means a more negative slope of the plot. This feature is used to analyse the temperature increase during the photo-crystallographic experiments as explain below.

During the photo-crystallographic experiments, the energy deposited by the laser pulse largely exceed the energy necessary for the LS to HS transition, which results in some heat diffusion and global warming. A modified Wilson plot, known as photo-Wilson plot (Figure S23-S26), is then used to estimate the lase-induced temperature increase due to heat dissipation, in a similar way as described above for the temperature-Wilson plots. From the photo-Wilson plot is possible to calculate the variation of the isotropic temperature factor between the laser-ON data sets and the laser-OFF data sets (ΔB^{ON-OFF})[5]:

$$ln\left(\frac{I^{ON}}{I^{OFF}}\right) = -2\Delta B^{ON-OFF}(\sin\theta/\lambda)^2 \qquad \text{(S3)}$$

where, I^{ON} and I^{OFF} are the observed intensities of the laser-ON and laser-OFF data sets at delay time. Note that both the thermal-Wilson plot and the photo-Wilson plot were brought to the same scale before calculating the value of ΔB. For more information about this topic, the reader is referred to the literature[5].

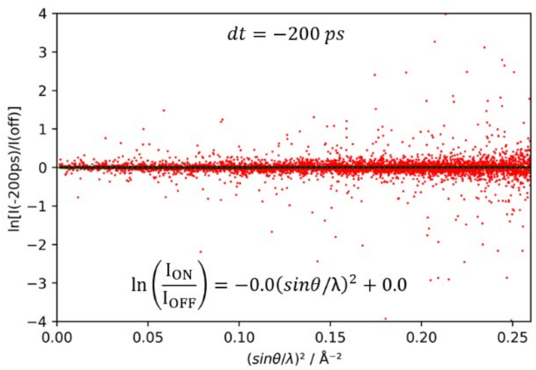

Figure S23. PhotoWilson plots of **FE4** for the reference data set dt<0.

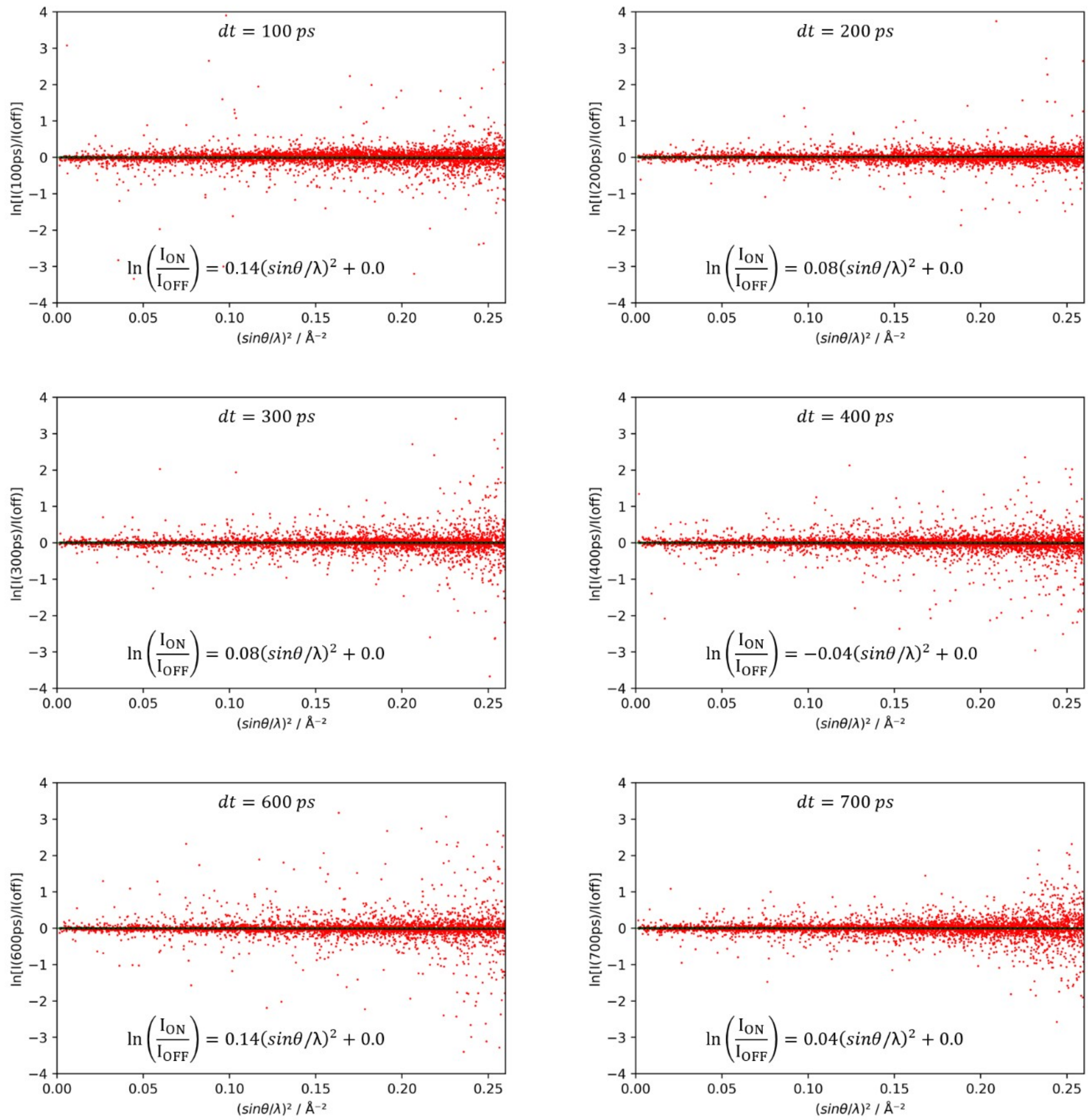

Figure S24. PhotoWilson plots of **FE4** during the photoinduced step.

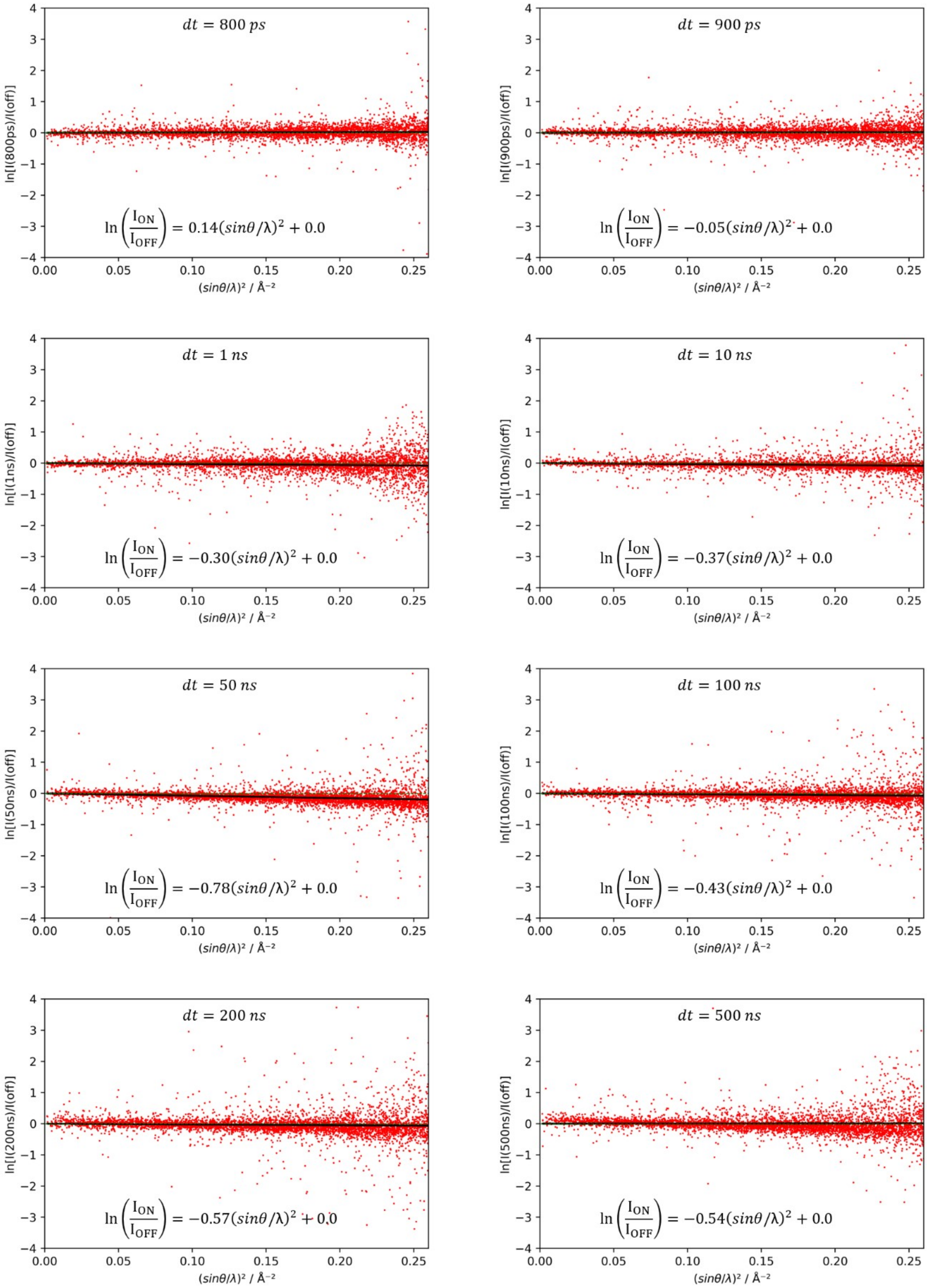

Figure S25 PhotoWilson plots of **FE4** during the elastic step.

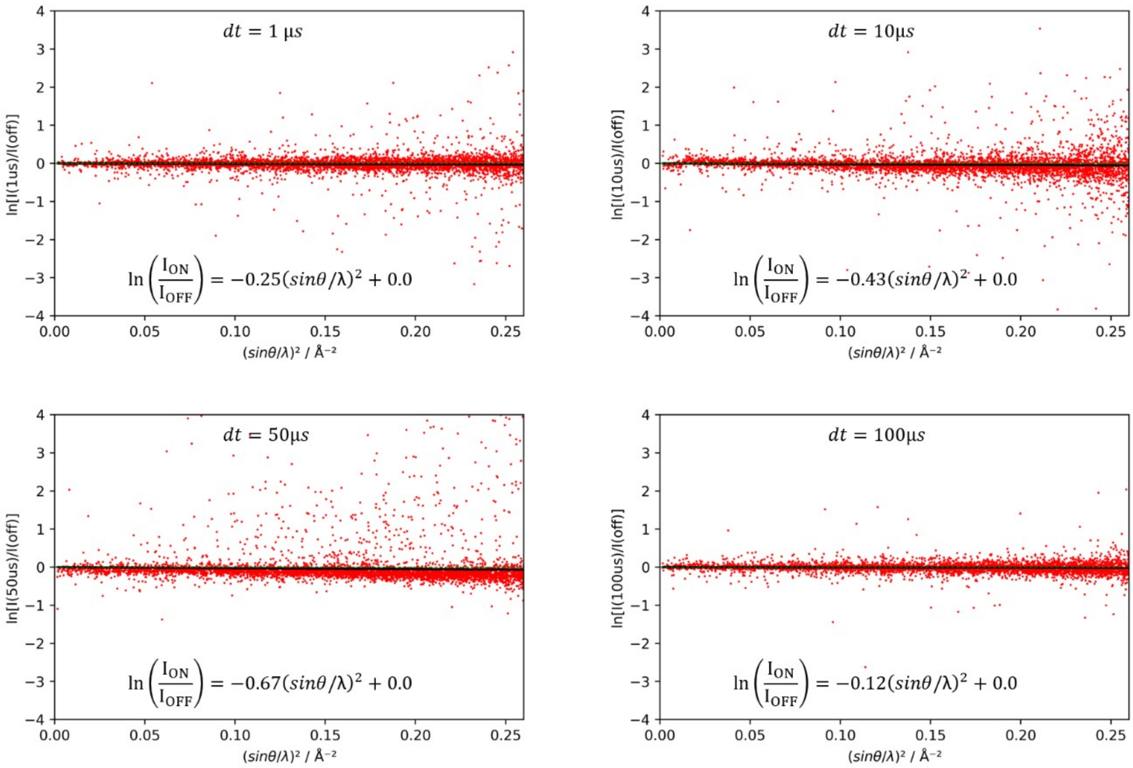

Figure S26 PhotoWilson plots of **FE4** during the thermal step.

References

1 B. Schneider, S. Demeshko, S. Neudeck, S. Dechert and F. Meyer, *Inorg. Chem.*, 2013, **52**, 13230–13237.

2 M. Marchivie, P. Guionneau, J.-F. Létard and D. Chasseau, *Acta Crystallogr. B*, 2005, **61**, 25–28.

3 M. Marchivie, P. Guionneau, J.-F. Létard and D. Chasseau, *Acta Crystallogr. B*, 2003, **59**, 479–486.

4 A. J. C. Wilson, *Nature*, 1942, **150**, 152–152.

5 M. S. Schmøkel, R. Kamiński, J. B. Benedict and P. Coppens, *Acta Crystallogr. A*, 2010, **66**, 632–636.